Thermochimica Acta, 142 (1989) 329–342
Elsevier Science Publishers B.V., Amsterdam – Printed in The Netherlands

THERMAL ANALYSIS OF CATALYST SURFACES

J.E. BAKER, R. BURCH * and S.E. GOLUNSKI

Catalysis Research Group, Department of Chemistry, University of Reading, Whiteknights, Reading RG6 2AD (Gt. Britain)

(Received 20 June 1988)

ABSTRACT

Surface characterization of a single sample of catalyst can be achieved through a sequence of related thermal techniques, all of which are carried out using the same equipment. The methods have been employed in a study of copper-based alcohol-synthesis catalysts.

Evolved gas analysis reveals the adsorbed contaminants on the surface of a calcined sample. Standard Cu–Zn–O catalysts have been found to yield CO_2, H_2O and NO as a result of the dissociation of surface hydrogencarbonates, carbonates and nitrogenous species. Limited temperature-programmed reduction usually shows the CuO component being reduced, but it provides no real indication of the resultant surface sites. However, the reduced surface can be probed by coadsorbing CO/H_2 or $CO/CO_2/H_2$; temperature-programmed desorption then allows active surface phases to be identified. The surface of a multicomponent catalyst was found to comprise Cu, ZnO and Al–Zn–O, but no cobalt phase was detected even though Co had been used as a precursor. Temperature-programmed heterogeneous reaction over reduced Cu–Zn–Co–O has shown that the appearance of higher alcohols corresponds to the decline in methanol formation, and suggests that the products are formed by consecutive reactions.

1. INTRODUCTION

Traditional forms of thermal analysis, such as thermogravimetry and differential thermal analysis, are particularly effective for detecting phase changes in catalyst precursors during drying and calcination [1]. When combined with methods of structural analysis, these techniques can be used to determine the stages in a complex series of transformations [2], but the information relates essentially to the bulk and so may only lead to some general predictions about the nature of the catalyst surface. Although there are other methods, e.g. microgravimetry [3], thermoelectrometry [4] and microcalorimetry [5], which are sensitive enough to allow surface changes to be monitored, the results can be difficult to interpret. However, by detecting

---

* Author to whom correspondence should be addressed.

0040-6031/89/$03.50

and identifying gaseous species desorbing from the surface of a solid sample, it is possible to achieve surface-specific thermal analysis.

In our current studies of copper-based catalysts, we carry out a sequence of related experiments using a single apparatus, in which the products of adsorption/desorption or heterogeneous reaction are analysed by quadrupole mass spectrometry [6] during programmed heating of a sample. The results provide information about the contaminants on the surface of calcined Cu–metal oxides, the different stages during the subsequent reduction, the active sites on the resultant supported metal catalysts and the mechanism of the heterogeneous catalytic reaction.

Our interest in supported copper arises from its ability to catalyse the conversion of CO/H_2 or $CO/CO_2/H_2$ to alcohols. In its simplest forms e.g. Cu/SiO_2 [7] or Cu/ZnO [8], it is used to generate methanol [9,10], but higher alcohols can be produced by adding a Fischer–Tropsch function to the catalyst [11]. Although a substantial number of investigations have been reported [9–11], many problems relating to the catalytic surface have yet to be resolved. These include the exact nature of the active sites, the role of the support material and the most likely interactions between the adsorbed species.

2. APPARATUS

A schematic diagram of the complete apparatus is shown (Fig. 1a) together with a more detailed representation of the gas supply system (Fig. 1b).

Helium and hydrogen (BOC Ltd) are used as the inert carrier gas and the reducing atmosphere, respectively. These gases are purified in two stages. On the high pressure side of the flow controller (Negretti and Zambra Ltd) oxygen is trapped by a commercial copper catalyst (BASF) which has been reduced under hydrogen at 525 K. Then, before reaching the reactor, the He or H_2 (at 1.01×10^5 Pa) passes through a cold trap (77 K) filled with molecular sieve (Sigma; 10 Å). The proportion of O_2 in the carrier/reducing gas entering the vacuum chamber is typically 5–10 ppm. However, as the reactor and tubing have not been baked, the H_2O background tends to be approximately 0.01%.

Gas mixtures, $CO/H_2 = 1:3$ and $CO/CO_2/H_2 = 1:1:8$ (BOC), are used as the adsorbates and the reactants. A pulse of adsorbate can be carried through the reactor by filling the sampling loop (1.9 cm^3 at 1.01×10^5 Pa) and then switching the gas sampling valve (Valco; p-type) so that the carrier gas is diverted through the loop. Prior to adsorption or reaction, the gases pass only through the molecular sieve (at 295 K), which removes H_2O and iron carbonyls.

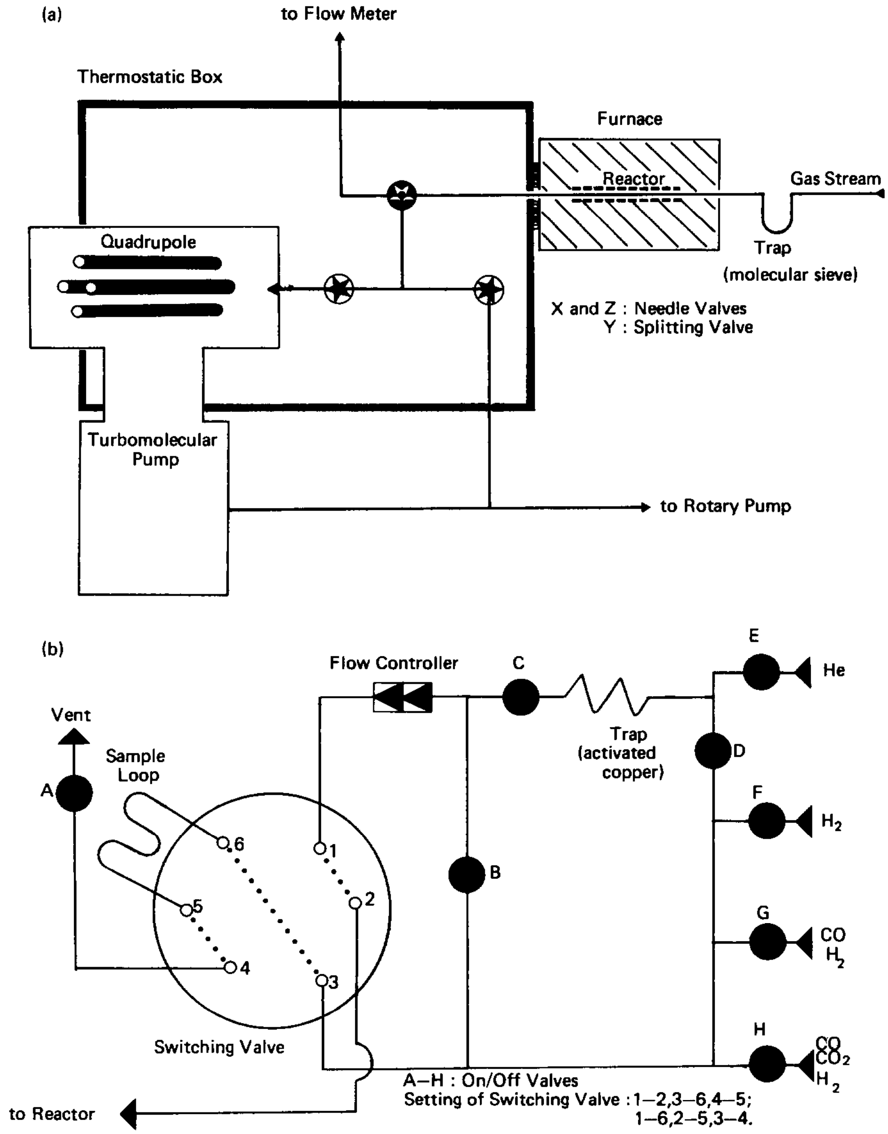

Fig. 1. (a) Apparatus used to identify evolved/desorbed gases during programmed heating of a catalyst sample. (b) Gas supply system.

A short cylindrical bed (diameter: 4 mm; length: 10–20 mm) of catalyst (250 mg) is held between two glass-wool plugs inside a glass-lined steel reactor (SGE Ltd). Although the lining limits the maximum temperature to 775 K, it prevents spurious effects arising from adsorption on the stainless steel [12]. The reactor is positioned within a horizontal tube furnace, which is controlled by a temperature programmer (Eurotherm; type 818). A thermocouple (NiCr–NiAl), fitted inside the furnace and lying adjacent to the reactor, detects the temperature in the immediate vicinity of the catalyst bed.

In order to minimize the delay between evolution/desorption of gaseous species and their detection, the reactor is linked to the vacuum chamber by a short length of capillary tubing, However, as the pressure inside the chamber must not exceed 6.6×10^{-3} Pa (the limit for the mass spectrometer filament), only a small fraction of the gas stream can be admitted. A splitting valve (SGE; type MCVT/100) allows either all the gas to be vented through a flow meter, or some of it to be sampled. The sample stream can be further divided by opening needle valves (SGE; type MCV/100) between the vacuum chamber and the rotary pump (Edwards; type E2M-1.5). Initially, the needle valves need to be carefully "balanced", so that selective pumping does not occur, but once set, they do not need to be adjusted routinely. The vacuum chamber, splitting valve, needle valves and capillary tubing are enclosed by a thermostatic box (375 K) to avoid condensation.

The turbomolecular pump (Edwards; type ETP 4/80) reaches its maximum rotational speed after 20 s, but it needs to be left running for several hours before a steady minimum pressure (approximately 2.5×10^{-6} Pa) can be achieved inside the vacuum chamber. Although strongly recommended [12] for its rapid pumping, a turbomolecular pump is not as effective as a diffusion pump for removing lighter gases. After completion of an experiment, the background spectrum often shows comparatively high partial pressures for H_2 and He, but these peaks can be quickly reduced by temporarily opening the gas ballast valve on the rotary pump.

The quadrupole mass spectrometer (Spectromass: type Dataquad 100-V3.15) can scan the range of 1–100 a.m.u., allowing even pentanol (and its isomers) to be detected during the course of alcohol synthesis reactions. In our experiments, the spectrometer is most often used to perform a trend analysis, in which up to eight peaks can be selected and repeatedly scanned, with their partial pressures being recorded as a function of time.

We have confirmed the reliability of the apparatus by examining the thermal decomposition of hydrated salts, and comparing the onset and peak temperatures to those found by thermogravimetry and differential thermal analysis under similar conditions.

3. TECHNIQUES

3.1. Evolved gas analysis (EGA)

3.1.1. Principle

EGA involves heating a sample, under an inert atmosphere, at a uniform rate. Gaseous products of dehydration [13], decomposition [14] or desorption [15] are identified, and their concentrations are plotted as a function of temperature. An EGA trace of a calcined catalyst can simply be used as a "fingerprint", i.e. it is characteristic of a particular formulation and method of preparation. More importantly, however, it can allow the nature of transient surface species to be deduced; these may be remnants of undissociated precursors, or molecules adsorbed by the catalyst during calcination or subsequent storage.

3.1.2. Method

We carry out EGA at a fixed heating rate of 10 K min^{-1}, mainly because it allows 4–8 peaks in the mass spectrum to be scanned with high precision at 2–5 K intervals, but also because our results can be compared with those obtained by standard techniques of thermal analysis, in which this heating rate is most frequently used. Throughout all our experiments, a constant gas flow rate (30 cm^3 min^{-1}) is used (see section 3.3.2.).

Wherever possible, unambiguous peaks in the mass spectrum are selected on the basis of prior knowledge of the catalyst preparation. For example, peaks associated with nitrogen oxides ($m/e = 30$ and 46), carbon dioxide ($m/e = 44$) and water ($m/e = 18$ and 17) are scanned, if a calcined catalyst has been prepared by precipitation of carbonate from a nitrate solution. For commercial catalysts, or those of unknown origins, it is worthwhile examining the complete spectrum at several temperatures before selecting peaks and carrying out EGA on a fresh sample.

3.1.3. Example: Cu–Zn–O

Figure 2 shows the EGA traces for two Cu–Zn–O catalysts, which had been prepared [16,17] by precipitating the mixed-metal carbonate from an aqueous solution of the nitrates. In both cases, the precursor had been dried and calcined, but different conditions had been used during calcination. One sample (A) had been heated (625 K; 3 h) in a muffle furnace [16]; the other (B) had been heated (675 K; 10 h) under a flowing atmosphere of O_2 [17].

During EGA, both samples yielded H_2O, CO_2 and NO (Fig. 2), as well as trace amounts of NO_2. From the relative sizes of the peaks, it is clear that the surface of sample B was much less contaminated with NO. It is also significant that, for sample A, a peak maximum for NO coincides with a maximum for CO_2. Coincident desorption generally indicates common surface species [18], but their nature is not immediately obvious in this case, and further investigation (e.g. by Fourier-transform IR) will be necessary. The simultaneous desorption of CO_2 and H_2O (375–495 K), from both samples, is easier to explain, because the proportions (after deducting the contribution from desorbing molecules of H_2O) suggest the dissociation of hydrogencarbonates

$$2HCO_3^-(surf) \rightarrow H_2O(g) + 2CO_2(g) + O^{2-}(surf) \qquad (1)$$

Sample B yielded H_2O and CO_2 above its calcination temperature. The former we attribute to the desorption of surface hydroxyl species [19],

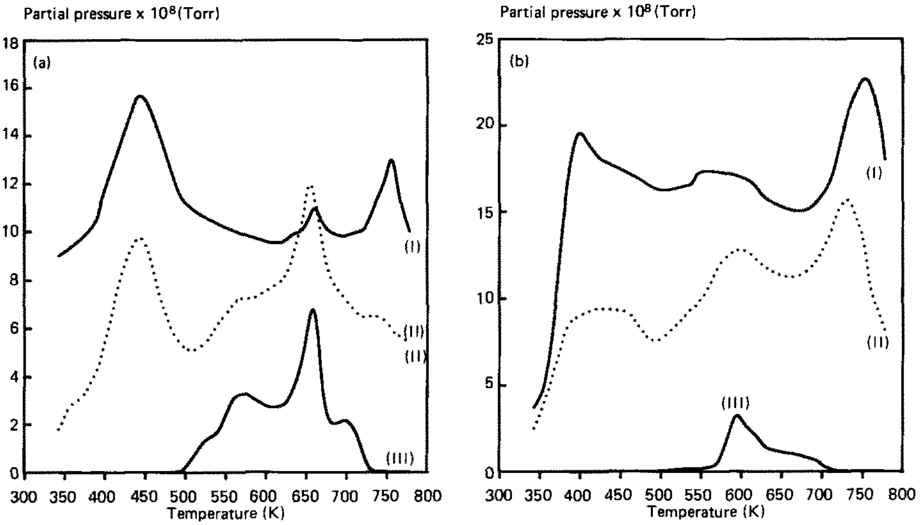

Fig. 2. EGA of Cu–Zn–O. (a) Sample calcined at 625 K in muffle furnace. (b) Sample calcined at 675 K under flowing oxygen. (I), $m/e = 18$ (H_2O); (II), $m/e = 44$ (CO_2); (III) $m/e = 30$ (NO). 1 Torr = 101325/760 Pa.

whereas the CO_2 peak is very similar, in shape and position, to one we have observed after adsorbing $CO/CO_2/H_2$ on reduced Cu–Zn–O. We believe that it is due to the dissociation of carbonate species, which are readily formed on the surface of ZnO [20].

In our work, an important function of EGA is as a means of determining when chemical stability of a catalyst surface is achieved. It is particularly effective for continuously monitoring the removal of the nitrogenous species, which can form inert nitrides during the reduction of Cu-based catalysts and prevent the adsorption of CO [21].

3.2. Temperature-programmed reduction (TPR)

3.2.1. Principle

Although the reduction of metal oxides can be studied by a number of methods [22–25], the term TPR is now often used in reference to techniques in which the consumption of hydrogen is monitored as a function of temperature. At its best, TPR can show the stages and extent of reduction, and so may lead to an accurate assignment of the phases present in both the calcined and the reduced forms of a catalyst [26]. However, if the results are considered in isolation, they can be very misleading, especially when

(a) hydrogen is consumed as a result of spillover from the metal onto the support [22],

(b) hydrogen is adsorbed/desorbed [26] and

(c) reduction gives rise to double or multiple peaks. (These may indicate the presence of two or more distinct chemical phases in the calcined sample, but could also be due to a mixture of particle sizes [25].)
An alternative is to detect the evolution of water, but this is not usually practised because processes other than reduction can yield H_2O.

3.2.2. *Method*

In carrying out TPR, we try to achieve the same degree of reduction as in the activation of industrial copper-based catalysts [27,28]. We use a slow heating rate (5 K min^{-1}), and then maintain the sample at the maximum temperature (525 K) until there are no further signs of reduction (usually after 1–2 h). To avoid some of the problems mentioned previously (section 3.2.1.), we monitor both the evolution of water and the consumption of hydrogen.

3.2.3. *Examples: Cu–Zn–O, Cu–Zn–Co–Al–O*

Our traces for Cu–Zn–O (Fig. 3a) show the reduction of CuO (extrapolated onset temperature = 387 K; T_p = 445 K). It is also clear that reduction is effectively complete before the maximum temperature is reached. This probably indicates that the bulk of Cu(II) has been reduced to Cu(0) [16], and so it may be inferred that the active catalyst is comprised of metallic copper supported on ZnO. However, TPR alone cannot indicate whether the surface contains Cu(0), Cu(I) or a mixture of both, nor whether the phases are segregated or interdispersed.

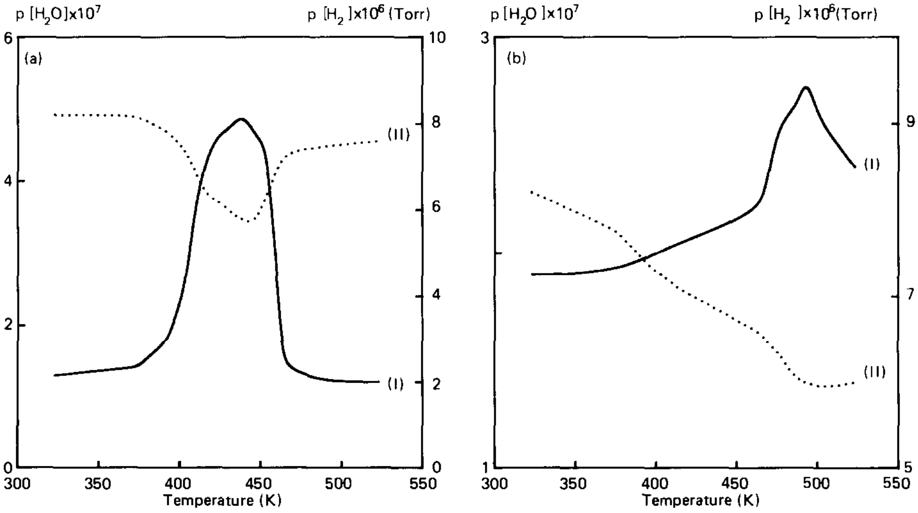

Fig. 3. TPR. (a) Cu–Zn–O. (b) Cu–Zn–Co–Al–O. (I), $m/e = 18$ (H_2O); (II), $m/e = 2$ (H_2). $p[H_2O]$ = partial pressure of H_2O; $p[H_2]$ = partial pressure of H_2.

TPR of a multicomponent catalyst (prepared by controlled co-precipitation of Cu–Zn–Co–Al hydroxycarbonate, followed by calcination at 775 K) shows that reduction occurs more gradually and is incomplete when the maximum temperature is reached (Fig. 3(b)). This example reveals the limitations of our form of TPR which, although non-destructive, provides few indications about the nature of what is probably a multi-phase surface.

3.3. Temperature-programmed desorption (TPD)

3.3.1. Principle

In many TPD experiments [12,29,30], a single gaseous adsorbate is brought into contact with a sample under isothermal conditions. Excess adsorbate is flushed away by an inert gas stream or removed by pumping. The temperature of the sample is then increased linearly and desorbing species are detected and identified.

A TPD trace shows the concentration of a desorbed species as a function of sample temperature. The number of peaks may indicate the number of different surface sites, or the number of different surface species formed as a result of adsorption. The activation energy for desorption (E_d) is related to T_p [31]

$$A/b \exp(-E_d/RT_p) = E_d/RT_p^2 \tag{2}$$

Therefore, E_d can be found from the variation in T_p with heating rate b or from a single TPD trace if the pre-exponential factor (A) is known. In practice, a "normal" value for A (10^{13} s^{-1} [31]) is often assumed [15,32,33], so allowing E_d to be estimated from T_p.

3.3.2. Method

A pulse of CO/H_2 or $CO/CO_2/H_2$ is carried, by the helium stream, through the bed of reduced catalyst (at 323 K). Although the pulse should resemble a square wave [12], by the time it is detected, it approximates to a triangular wave. After adsorption, the mass spectrum is monitored until all peaks have returned to their background levels (after 15–20 min). Usually, the peaks at $m/e = 2$, 18, 28 and 44 are then selected, and a trend analysis is performed as the catalyst is heated. A fairly high heating rate (30 K min^{-1}) has been chosen, because it falls within the range (0.3–1.0 K s^{-1}) most often used in TPD studies of similar catalysts [15,18,19,32].

Our gas flow rate (30 cm^3 min^{-1}) was chosen as a result of preliminary TPD experiments. Due to our concern about possible contamination of the catalysts during their prolonged exposure to a gas stream, we started by using very low flow rates. After incorporating efficient traps into the design of the apparatus, we increased the flow until further slight changes had no effect upon the shape of the peaks in our TPD traces [12].

3.3.3. *Example: "Cu-Zn-Co-Al-O"*

Figure 4 shows the resultant TPD traces after dosing an activated multicomponent catalyst with $CO/CO_2/H_2$. The desorption of CO_2 clearly coincides with most of the desorption of H_2. Distinct maxima for both molecules (and for CO) occur at 585 K, and peaks are also discernible at 443 and 623 K, from which we estimate E_d to be 162, 123 and 172.5 kJ mol^{-1}, respectively (assuming "normal" A). The simultaneous desorption of CO_2 and H_2 (and in some cases CO [15,34]), from related catalysts, has been attributed [15,18,30,34] to the dissociation of surface methanoate (formate). Indeed, it has been shown that CO_2 and H_2 are yielded simultaneously following the adsorption of methanoic (formic) acid on copper [30].

The peak temperatures, for the three stages of coincident desorption, agree closely with values reported for Cu (440 K [18,34]), ZnO (580–590 K [15,34]) and Al–Zn–O (610–620 K [34]). However, there are no apparent

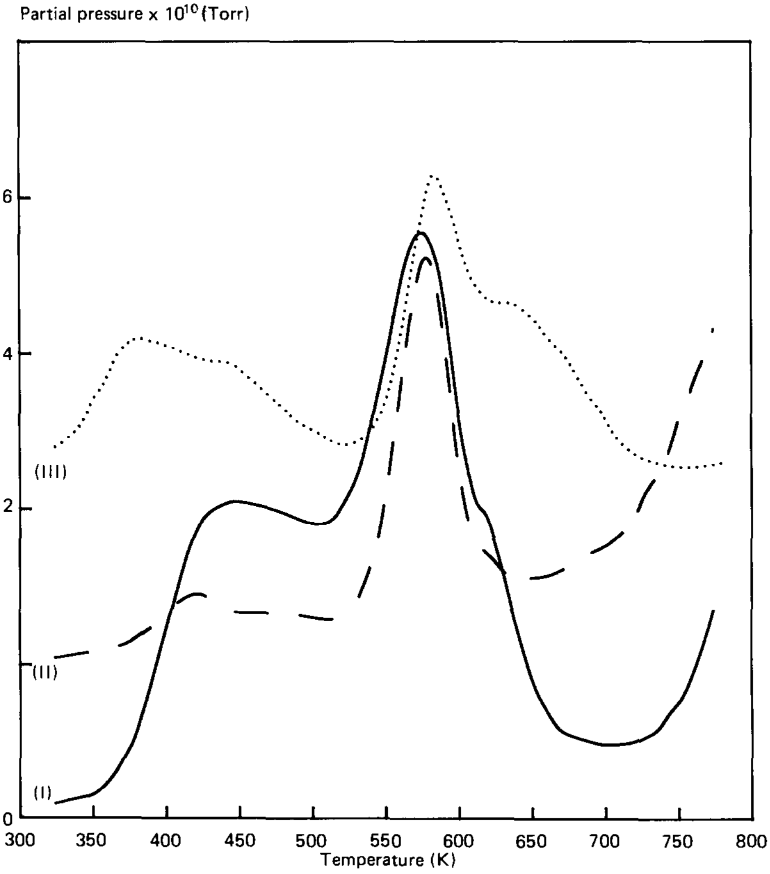

Fig. 4. TPD, after co-adsorption of $CO/CO_2/H_2$ on Cu-Zn-Co-Al-O at 323 K. (I), $m/e = 44$ (CO_2); (II) $m/e = 28$ (CO); (III), $m/e = 2$ (H_2).

peaks due to cobalt sites, which (from our studies of Cu–Zn–Co–O) we believe give rise to coincident desorption at 685 K. It appears, therefore, that the catalyst surface contains three distinct phases; possibly in the form of copper particles supported on zinc aluminate, within a matrix of zinc oxide. Such an array of surface sites would also account for the results of subsequent activity/selectivity tests, which have shown the catalyst to be mainly effective for the synthesis of methanol (and not higher alcohols, as would be expected for supported Cu–Co). Furthermore, chemical analysis (by atomic absorption) has indicated a very low cobalt content in the bulk. We have traced the problem back to the first stage of catalyst preparation, in which a hydrotalcite-type structure, i.e. $M_6^{2+}M_2^{3+}(OH)_{16}CO_3 \cdot 4H_2O$ [11], is precipitated by adding aqueous sodium carbonate to a solution of the metal nitrates. If the pH is not carefully controlled (within the range 7–9), sequential precipitation may occur and the other components can be removed before the Co-phase has been precipitated.

It is also worth mentioning that our TPD technique could be described as temperature-programmed reaction spectroscopy (TPRS [12]), because it involves the co-adsorption of different types of molecules, which interact on the surface of the sample. An important advantage of this technique is that the adsorbates are the reactants in the heterogeneous reaction, and so the sites identified are likely to be catalytically active.

3.4. Temperature-programmed heterogeneous reaction (TPHR)

3.4.1. Principle

We use the term TPHR to denote an experiment in which the products of a heterogeneously catalysed reaction are monitored, while a sample is heated under a stream of reactant gases. (Other authors refer to the technique simply as temperature-programmed reaction [12,22], but this can lead to confusion, especially if abbreviated.)

One application of TPHR is for assessing the potential of a catalyst, prior to more detailed testing of its activity and selectivity. More fundamentally, the technique can provide information about the mechanism for the formation of products and by-products. However, interpretation of the data may not always be straightforward. For example, the decay of a peak in a TPHR trace does not necessarily reflect either a decline in catalytic activity or the onset of a consecutive reaction, but may indicate the limit of thermal stability of the particular product.

3.4.2. Method

In common with EGA, a heating rate of 10 K min^{-1} is used to enable several peaks in the mass spectrum to be accurately scanned. In most cases we select peaks associated with alcohols ($m/e = 31$, $-CH_2OH$ fragment) methane ($m/e = 15$, $-CH_3$ fragment) and water, as well as those due to specific products we expect to be formed. For novel catalysts, it is sometimes preferable to record the whole spectrum at a limited number of temperatures.

TPHR can lead to definite and irreversible changes in the composition and structure of a catalyst surface, and so it is the last technique we employ. For example, in carrying out the experiment on a supported metal under CO/H_2, the catalyst is subjected to reducing conditions in excess of those used during activation or even during the catalytic reaction; reduction of the support may occur, with new metal or alloy sites being created.

3.4.3. Example: Cu–Zn–Co–O

In studying the synergy between copper and cobalt, we prepared a catalyst by impregnating Cu–Zn–O with aqueous cobalt(II) nitrate and then drying, milling and calcining (775 K; 4h); the cobalt content of the resultant mixed-metal oxide was 5% (w/w). The catalyst was activated (EGA; TPR), before it was heated under $CO/CO_2/H_2$.

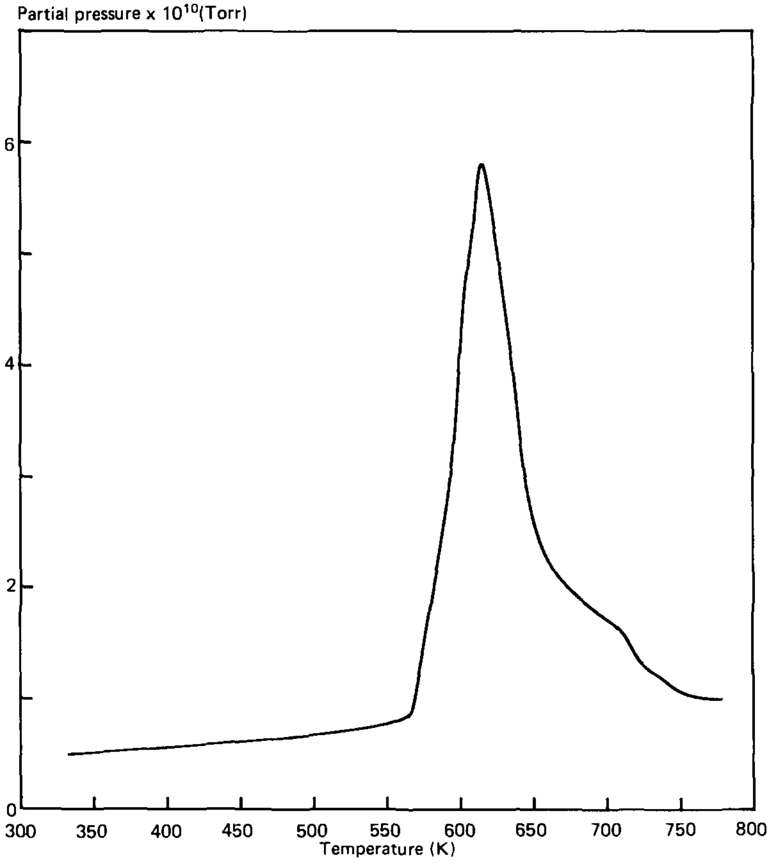

Fig. 5. TPHR of $CO/CO_2/H_2$ over Cu-Zn-Co-O. $m/e = 31$ (alcohols).

Initially, only one alcohol peak ($m/e = 31$) in the mass spectrum was scanned. The TPHR trace (Fig. 5) shows alcohol formation commencing at around 560 K, and reaching a maximum at 610 K, before declining in two steps. The experiment was repeated using a fresh activated sample, but the complete mass spectrum was monitored during much slower heating. It became apparent that the main alcohol peak is due to methanol, but as it recedes so higher alcohols (mainly butan-1-ol) are formed. These observations can be explained by the consecutive reactions

(a) adsorption and interaction of $CO/CO_2/H_2$ to form methanoate (HCOO) species,

(b) reaction of HCOO with adsorbed hydrogen

$$HCOO(ads) + 2H(ads) \rightarrow CH_3O(ads) + O(ads)$$

then either

(c) formation of methanol

$$CH_3O(ads) + H(ads) \rightarrow CH_3OH(g)$$

or

(d) further reaction with methanoate and/or other reactive intermediates to yield higher alcohols.

This scheme conflicts with a tentative mechanism [11], in which higher alcohols are formed by the insertion of CO into an alkyl chain.

4. CONCLUDING REMARKS

In common with other forms of thermal analysis, the results of these techniques are most meaningful when considered collectively. Although we have chosen different examples to illustrate the application of each method, all the catalysts mentioned have been subjected to the complete sequence of experiments.

Apart from characterizing the surface of freshly prepared samples, other studies are possible. For example, by carrying out TPD and TPHR on fresh and aged samples, it may be possible to determine the phase changes resulting from prolonged catalytic use. Similarly, the causes of deactivation can be investigated by regenerating the surface; for example, deposited carbon can be removed by heating the used catalyst under hydrogen [35] (this method is sometimes referred to as temperature-programmed surface reaction [12]). With slight modification, the apparatus can be used for transient kinetic experiments [36] (in mechanistic studies) or for reactive frontal chromatography [37] (to measure metal surface areas).

Finally, it is clear that the apparatus and the techniques can be used to examine other surface-dependent systems (such as ion-exchange materials [38]), and should not be limited to catalytic studies alone.

ACKNOWLEDGEMENTS

We thank the SERC for the awards of a studentship (to JEB) and a fellowship (to SEG).

REFERENCES

1 J.H.R. Ross, Anal. Proc. (London), 22 (1985) 239.
2 S.E. Golunski, T.G. Nevell and D.J. Hucknall, J. Catal., 88 (1984) 448.
3 G.E. Vrieland, J. Catal., 111 (1988) 14.
4 W.W. Wendlandt, Thermochim. Acta, 73 (1984) 898.
5 B. Fubini, V. Bolis and E. Giamello, Thermochim. Acta, 85 (1985) 23.
6 P.E. Miller and M.B. Denton, J. Chem. Educ., 63 (1986) 617.
7 S.A. Selim, H.A. Hassan, M. Abd-El-Khalik and R.Sh. Mikhail, Thermochim. Acta, 45 (1981) 349.
8 P. Porta, S. De Rossi, G. Ferraris, M. Lo Jacono, G. Minelli and G. Moretti, J. Catal., 109 (1988) 367.
9 J.C.J. Bart and R.P.A. Sneeden, Catalysis Today, 2 (1987) 1.
10 G.C. Chinchen, P.J. Denny, J.R. Jennings, M.S. Spencer and K.C. Waugh, Appl. Catal., 36 (1988) 1.
11 Xu Xiaoding, E.B.M. Doesburg and J.J.F. Scholten, Catalysis Today, 2 (1987) 125.
12 J.L. Falconer and J.A. Schwarz, Catal. Rev. Sci. Eng., 25 (1983) 141.
13 F. Paulik and J. Paulik, Analyst, 103 (1978) 417.
14 M.R. Holdiness, Thermochim. Acta, 75 (1984) 361.
15 M. Bowker, H. Houghton and K.C. Waugh, J. Chem. Soc., Faraday Trans. 1, 77 (1981) 3023.
16 G.J.J. Bartley and R. Burch, Appl. Catal., 28 (1986) 209.
17 R. Burch and R.J. Chappell, Appl. Catal., 45 (1988) 131.
18 M. Bowker, R.A. Hadden, H. Houghton, J.N.K. Hyland and K.C. Waugh, J. Catal., 109 (1988) 263.
19 D. Chadwick and P.J.R. O'Malley, J. Chem. Soc. Faraday Trans. 1, 83 (1987) 2227.
20 K. Atherton, G. Newbold and J.A. Hockey, Discussions of the Faraday Society, No. 52, The Faraday Society (London), 1972, p. 33.
21 V. Higgs and J. Pritchard, Appl. Catal., 21 (1986) 149.
22 G.C. Bond and M.R. Gelsthorpe, Therm. Anal. Abstr., 14 (1985) 205.
23 S. Gusi, F. Trifiro and A. Vaccari, Reactivity of Solids, 2 (1986) 59.
24 E.R.A. Matulewicz, M.S. de Keijser, J.C. Mol and F. Kapteijn, Thermochim. Acta, 72 (1984) 111.
25 N.W. Hurst, S.J. Gentry, A. Jones and B.D. McNicol, Catal. Rev. Sci. Eng., 24 (1982) 233.
26 Y.-J. Huang, J. Xue and J.A. Schwarz, J. Catal., 111 (1988) 59.
27 Mitsubishi Gas Chemical Co. Inc. (Japan), U.K. Patent No. 2047556 B, 1983.
28 Institut Français du Petrole (France), U.K. Patent No. 2158730 A, 1985.
29 R.J. Cvetanovic and Y. Amenomiya, Adv. Catal., 17 (1967) 103.
30 R.J. Madix, Adv. Catal., 29 (1980) 1.
31 F.C. Tompkins, Chemisorption of Gases on Metals, Academic Press, London, 1978, p. 63.
32 D.L. Roberts and G.L. Griffin, J. Catal, 110 (1988) 117.
33 R.A. Hadden, H.D. Vandervell, K.C. Waugh and G. Webb, Catal. Lett., 1 (1988) 27.
34 H. Idriss, Ph.D. thesis, Universitè Louis Pasteur de Strasbourg, 1987, p. 58.

35 J.G. McCarty and H. Wise, J. Catal., 57 (1979) 406.
36 F.J.J.G. Jansenn, F.M.G. van den Kerkhof, H. Bosch and J.R.H. Ross, J. Phys. Chem., 91 (1987) 5921.
37 G.C. Chinchen, C.M. Hay, H.D. Vandervell and K.C. Waugh, J. Catal., 103 (1987) 79.
38 S.E. Golunski, K.D. Helps and M.J. Hudson, to be published.